# Interaction between Cytochrome *c* and Cytochrome *c* Peroxidase: Excited-State Reactions of Zinc- and Tin-Substituted Derivatives†

H. Koloczek,‡ T. Horie,§ T. Yonetani, H. Anni, G. Maniara, and J. M. Vanderkooi*
*Department of Biochemistry and Biophysics, School of Medicine, University of Pennsylvania, Philadelphia, Pennsylvania 19104*
*Received July 29, 1986; Revised Manuscript Received December 22, 1986*

ABSTRACT: The effect of cytochrome *c* peroxidase (CCP) and apoCCP on the fluorescence and phosphorescence of Zn and Sn cytochrome *c* (cyt *c*) and the effect of cyt *c* on the fluorescence and phosphorescence of Zn CCP were examined. We found the following: (1) The fluorescence yields of Zn and Sn cyt *c* were quenched by about 20% by CCP, consistent with energy transfer between the two chromophores with a separation of about 1.8 nm. (2) The phosphorescence spectrum of Zn cyt *c* (but not Sn cyt *c*) shifts by 20 nm to the blue upon complexation with either CCP or apoCCP; at the same time the phosphorescence lifetime of Zn cyt *c* decreases from 12 ± 2 to 6 ms with apoCCP addition. Zn CCP phosphorescence decay increases from 8.3 to 9.1 ms upon addition of poly(L-lysine) used to mimic cyt *c*. It is concluded from these results that binding of the redox partner or an analogue to Zn CCP and Zn cyt *c* results in a conformational change. (3) The respective phosphorescence lifetimes of Zn and Sn cyt *c* were 13 and 3 ms in the absence of CCP and 1.6 and 1.1 ms in the presence of CCP; this corresponds to a quenching rate due to CCP of 519 and 570 $s^{-1}$, for Zn and Sn cyt *c*, respectively. The phosphorescence of Zn CCP is also affected by native cyt *c* but is dramatically less than the complementary pair; the quenching rate constant is 17 $s^{-1}$. (4) Poly(L-aspartate) decreased the phosphorescence lifetime of Zn cyt *c* and Sn cyt *c*; this result appears to be due to interaction between closely bound cyt *c* derivatives. It is concluded that electron transfer (or exchange) occurs between the excited triplet state of metal derivatives of cyt *c* or CCP and closely bound porphyrins. In addition, there are conformational effects induced by binding of the redox partner.

The complex between CCP[1] and cyt *c* represents one of the best studied of all redox pairs involving heme proteins and is one of a few redox pairs in which the three-dimensional structure of each of the partners has been determined (Poulos et al., 1980; Takano et al., 1973). As a tool to study these heme proteins, several groups have prepared derivatives in which iron has been replaced by zinc or other closed-shell metals (Yonetani & Asakura, 1968; Vanderkooi et al., 1976). The porphyrins in these protein derivatives, unlike the parent hemes, are fluorescent and phosphorescent and can serve as reporters of the heme site.

Conceptually, excited states can be considered as electronic isomers of the ground state with the difference that both singlet and triplet excited-state molecules are more reactive than the ground-state molecule. Specific interactions between excited-state molecules and neighboring molecules include Coulombic interactions (through space) and electron-exchange and -transfer reactions (requiring orbital overlap) (Turro, 1978). Coulombic interactions serve as a means to study the heme distances (Vanderkooi et al., 1977), whereas electron-exchange/transfer reactions provide a kinetic means to study how the protein and neighboring hemes influence the kinetics of relaxation from excited to ground states (Zemel & Hoffman, 1981; Simolo et al., 1984; Ho et al., 1985; McLendon & Miller, 1985; Cheung et al., 1986; Peterson-Kennedy et al., 1986).

The conformational and electronic interactions between CCP and cyt *c* were studied in closed-shell metal derivatives. Two ions were substituted for iron in cyt *c*: Zn, which is 2+ charged, the same charge as ferrous iron, and Sn, which is 4+ charged. In addition to different charges these two derivatives have different emission spectra and fluorescent and phosphorescent lifetimes (Vanderkooi et al., 1976; Dixit et al., 1984), and therefore, they are expected to respond differently to CCP because the overlap integrals are different. The decay properties of the singlet excited state were monitored by fluorescence lifetime, spectra, and intensity measurements. The properties of the triplet state were examined either by phosphorescence or by delayed fluorescence, the latter arising from thermal equilibration of the triplet state with the singlet state (Dixit et al., 1984). We also report on the interaction between cyt *c* molecules under conditions when the molecules are close together, i.e., bound to poly(L-aspartate).

The luminescence properties of porphyrins indicate conformational interactions between the polypeptide chains of CCP and cyt *c* and electronic interactions between the neighboring porphyrins.

## Materials and Methods

*Materials.* Type III and type VI horse heart cyt *c*, glucose, coproporphyrin I, glucose oxidase (type VII), poly(L-lysine) (approximate $M_r$ 25000), poly(L-aspartate) (approximate $M_r$ 20000), and catalase (bovine liver) were obtained from Sigma Chemical Co. (St. Louis, MO). Other reagents were of analytical grade. Distilled and deionized water was used throughout.

Sn cyt *c* and Zn cyt *c* were prepared from type III cyt *c* as previously described (Vanderkooi et al., 1976). Type VI cyt *c* was used when Fe cyt *c* is indicated. CCP was prepared from bakers' yeast according to the procedure of Yonetani and Ray

† This work was supported by NIH Grant GM 34448 (J.M.V.) and NSF Grants PCM 83-16935 (T.Y.) and PCM 84-00844 (J.M.V.).
* Address correspondence to this author.
‡ Permanent address: Jagiellonian University, Krakow, Poland.
§ Permanent address: Tokyo College of Pharmacy, 1432-1 Horinauchi, Hachioji, Tokyo, Japan.

[1] Abbreviations: cyt *c*, cytochrome *c*; Zn cyt *c*, cytochrome *c* in which the iron was replaced by Zn; Sn cyt *c*, cytochrome *c* in which the iron was replaced by Sn; CCP, cytochrome *c* peroxidase; Zn CCP, cytochrome *c* peroxidase in which the iron protoporphyrin IX was replaced by Zn protoporphyrin IX; apoCCP, apoprotein moiety of CCP; apocyt *c*, apoprotein moiety of cyt *c*.

0006-2960/87/0426-3142$01.50/0 

(1965). Zn protoporphyrin IX was prepared from protoporphyrin IX as described by Leonard et al. (1974), and reconstitution of apoCCP with Zn protoporphyrin IX was carried out as described previously (Yonetani, 1967).

*Methods.* The detection of delayed fluorescence and phosphorescence depends critically upon removing $O_2$ from the sample. Oxygen was removed by including glucose oxidase (75 μg/mL), catalase (12.5 μg/mL), and 0.3% glucose in the sample, layering with mineral oil, and capping the cuvette (Dixit et al., 1984). Since residual oxygen or other impurities in the medium can cause quenching of phosphorescence, Zn coproporphyrin I was used as a standard, so that measurements using different buffers can be compared. Zn coproporphyrin I was prepared by stoichiometric addition of $ZnCl_2$ to coproporphyrin I at pH 8.0. The sample was diluted to an optical density of 0.14 at 406 nm in 20 mM phosphate, pH 7.0, and enzyme systems described above were added. At 20 °C, a lifetime of 3.9 ms was obtained; this lifetime was essentially the same in all the buffers used in this study. For prompt fluorescence spectra, $O_2$ was not removed from the sample.

Prompt fluorescence spectra and intensity were obtained with a Perkin-Elmer 650 spectrofluorometer. A Perkin-Elmer LS-5 spectrofluorometer was used to measure delayed fluorescence and phosphorescence spectra and their decay profiles. The instruments were equipped with red-sensitive Hammamatsu 928 photomultipliers. Decay profiles of phosphorescence and delayed fluorescence were analyzed with single- and double-exponential functions by a nonlinear fitting routine. The temperature for measurement was 20 °C except where indicated. The absorption spectrum of the sample was taken before and after phosphorescence measurement, and no evidence of a change in absorption was evident.

Fluorescence lifetime measurements used an excitation wavelength of 548 nm from a mode-locked argon laser pumping a cavity-dumped tunable dye laser. An emission monochromator was used to avoid Raman and other scattering artifacts. Fluorescence decay was followed by photon counting and computer fit by nonlinear analysis to a single-, double-, or triple-exponential decay function.

*Calculation of Coulombic Interactions.* Förster theory was used to calculate distances between donor and acceptor (Förster, 1959). The distance $R_0$ between donor and acceptor for which the energy-transfer and fluorescence rates are equal is given by

$$R_0^6 = (8.8 \times 10^{-5})\kappa^2 n^{-4} \Phi_D \int_0^\infty \epsilon_A(\lambda) f_D(\lambda) \lambda^4 \, d\lambda \quad (1)$$

where $\kappa$ is the dipole–dipole orientation factor, $n$ is the refractive index of the medium, $\epsilon_A$ is the extinction coefficient of the acceptor, $f_D$ is the normalized fluorescence intensity of the donor, and $\Phi_D$ is the fluorescence quantum yield of donor. The value of $\kappa$ was taken to be $^2/_3$; because the chromophores approximate $D_{4h}$ symmetry and $\kappa^2$ is proportional to $R_0^6$, errors in $\kappa^2$ will not greatly affect $R_0$ (Vanderkooi et al., 1980; Dale et al., 1979). The refractive index $n$ was taken to be 1.4. When the energy transfer efficiency $E$ is defined as

$$E = (1 - F_{donor})/F \quad (2)$$

where $F_{donor}$ and $F$ are the fluorescence intensities in the presence and absence of acceptor, respectively, then the distance $R$ between the chromophores is

$$R = (E^{-1} - 1)^{1/6} R_0 \quad (3)$$

and the rate of transfer is

$$k_q^f = \frac{1}{\tau_D}\left(\frac{R_0}{R}\right)^6 \quad (4)$$

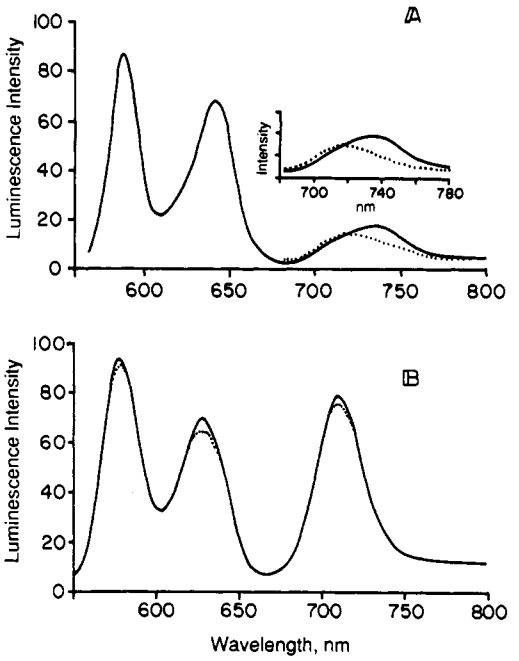


FIGURE 1: Delayed luminescence spectra of Zn cyt c and Sn cyt c. (A) (—) 10 μM Zn cyt *c*; (···) plus 20 μM CCP. (Inset) (—) 15 μM Zn cyt *c*; (···) plus 30 μM apoCCP. Excitation at 410 nm. (B) (—) 10 μM Sn cyt *c*; (···) plus 10 μM CCP. Excitation at 405 nm; Spectral slitwidths 10 nm; 20 mM potassium phosphate, pH 7.0; temperature 22 °C; gate time 1 ms; delay time 0.1 ms.

where $\tau_D$ is the observed lifetime in the absence of acceptor.

## RESULTS

*Luminescence of Zn and Sn Cyt c in the Presence of CCP.* The luminescence of Zn cyt *c* and Sn cyt *c*, attributable to prompt fluorescence, phosphorescence, and delayed fluorescence, was examined after addition of CCP and apoCCP. In Figure 1, the delayed luminescence spectra of Zn cyt *c* and Sn cyt *c* at room temperature are presented. In the case of Zn cyt *c*, the spectrum of the delayed fluorescence, with maxima at 588 and 648 nm, was not detectably altered by the addition of apoCCP or CCP (Figure 1A). The phosphorescence maximum of Zn cyt *c* at 738 nm was shifted to 718 nm upon addition of CCP or apoCCP (Figure 1A and inset). No effect of apoCCP or CCP was observed on the phosphorescence and delayed fluorescence spectrum of Sn cyt *c* (Figure 1B).

The prompt fluorescence spectrum of Zn cyt *c* was not affected by the addition of CCP (not shown), but the intensity decreased by about 20%, whereas the addition of apoCCP had almost no effect (Figure 2A, inset). The decay of phosphorescence of Zn cyt *c* was approximated by a single-exponential function with a lifetime of 12 ± 2 ms in the absence of CCP (Figure 2A). In the presence of CCP two components were evident in the decay profile: the short component had a lifetime of 1.6 ± 0.2 ms, whereas the long component had a lifetime corresponding to that of free Zn cyt *c*. As the concentration of CCP increased, the lifetime of the short component predominated. ApoCCP reduced the phosphorescence lifetime of Zn cyt *c* to a lesser extent than the native enzyme: at excess concentrations of apoCCP the lifetime was 6 ± 0.3 ms (Figure 2B). The observed lifetimes of phosphorescence were not detectably different from the delayed fluorescence ones, either in the absence or in the presence of CCP, as expected for delayed fluorescence resulting from the thermal repopulation of the singlet state from the triplet state (Parker & Hatchard, 1961). The quenching of Zn cyt *c* phosphorescence by CCP and apoCCP was independent of

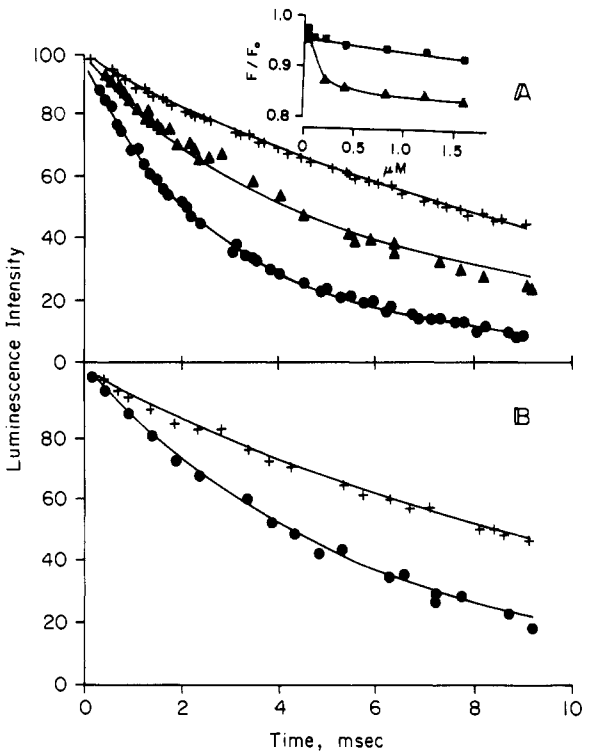


FIGURE 2: Effect of CCP and apoCCP on prompt fluorescence intensity and decay of delayed luminescence of Zn cyt c at room temperature. All solutions contained 20 mM phosphate buffer, pH 7.0. (A) 10 $\mu$M Zn cyt *c* (+), solid line is the computer best fit to the data for a single exponential with a lifetime of 12.9 ms (SE 0.004); same plus 3.3 $\mu$M CCP (▲), solid line is the computer fit to a two-exponential decay function with a lifetime of 12.9 ms and amplitude of 0.4 and a lifetime of 1.8 ms and amplitude of 0.6; 10 $\mu$M Zn cyt *c* and 10 $\mu$M CCP (●), solid line is the computer fit to two decay functions with lifetimes of 12.9 and 1.85 ms and amplitudes of 0.2 and 0.8, respectively. (Inset) Fluorescence intensity ($F/F_0$) of 0.56 $\mu$M Zn cyt *c* and CCP (▲) or apoCCP (■). (B) Decay of 10 $\mu$M Zn cyt *c* in the absence (+) and presence of 20 $\mu$M apoCCP (●) with the solid line representing the computer best fit of 12.5 and 6.1 ms, respectively. Excitation wavelength 549 nm; emission wavelength 588 nm; gate time 0.2 ms.

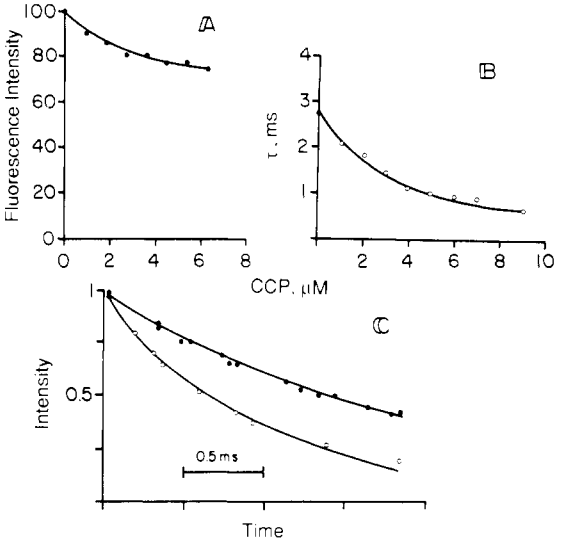


FIGURE 3: Effect of CCP on prompt fluorescence and decay of delayed luminescence of Sn cyt c at room temperature. The sample was 3.8 $\mu$M Sn cyt *c* in 1 mM potassium phosphate buffer, pH 7.0. (A) Prompt fluorescence intensity was observed at 577 nm with 405 nm as excitation wavelength. Inner filter absorption was corrected as described by Calhoun et al. (1983). (B) Sn cyt *c* phosphorescence lifetime: excitation at 405 nm; emission at 710 nm; gate time 0.5 ms. (C) Phosphorescence decay of Sn cyt *c* in the absence (●) and presence of 8 $\mu$M CCP (○). Solid lines are the computer fits to a single-exponential decay function with a lifetime of 3.0 and 1.1 ms, respectively.

buffer concentration in the range of 1–20 mM phosphate and independent of pH, between 6 and 7. On the other hand, the quenching effect was reversible after addition of 0.6 M KCl (not shown), a condition that causes the dissociation of the cyt *c*–CCP complex. The phosphorescence lifetime of Zn cyt *c* was not dependent upon the KCl concentration in the absence of CCP.

Similarly to Zn cyt *c*, the prompt fluorescence intensity of Sn cyt *c* decreased by ≥20% upon addition of CCP; the quenching profile followed a normal saturation curve, and quenching was maximal at 1:1 molar concentrations of the proteins (Figure 3A). The mean single phosphorescence lifetime decreased upon addition of CCP (Figure 3B), but the data were not sufficiently accurate to resolve it into two exponential functions. The lifetime was 3.0 ± 0.2 ms in the absence of CCP and 1.1 ± 0.1 ms at saturating concentrations of CCP (Figure 3C).

The fluorescence decays of Zn and Sn cyt *c* are both non single exponential (Figure 4). Addition of CCP reduces the lifetime; for example, the longest component of the decay of Sn cyt *c* was 1.7 ns in the absence of CCP and 1.1 ns in the presence of CCP (Figure 4B,C). The longest lifetime of Zn cyt *c*, 3.8 ns in the absence of CCP, was also proportionately reduced upon addition of CCP (not shown). The reasons for the nonexponential decay of fluorescence are unknown; however, the fluorescence decay data support the steady-state measurement (compare with Figure 2 inset and Figure 3A) that CCP acts as an acceptor for the prompt fluorescence of Zn and Sn cyt *c*.

*Luminescence of Zn and Cyt c in the Presence of Poly*(L-*aspartate*). Models of CCP and cyt *c* based upon X-ray analysis suggest that cyt *c* interacts with CCP by binding through lysine residues to aspartate residues on CCP (Poulos & Kraut, 1980). Therefore, poly(L-aspartate) was used to mimic the electrostatic effect of CCP. Addition of excess (not shown) or substoichiometric amounts (1:2) of poly(L-aspartate) to Zn cyt *c* and Sn cyt *c* results in quenching of the prompt fluorescence and a decrease in the phosphorescence and delayed fluorescence lifetimes by about 20% (Figure 5). Unlike the effect of CCP or apoCCP on Zn cyt *c*, the quenching of Zn cyt *c* phosphorescence in the presence of poly(L-aspartate) occurred without a detectable shift in the emission spectrum.

At much lower ratios of poly(L-aspartate) to Zn cyt *c* or Sn cyt *c* (1:50), dramatic quenching of phosphorescence occurred that was relieved by additional poly(L-aspartate) (Figure 5B). In the same concentration range, a smaller decrease in prompt fluorescence occurred, which did not exactly parallel the phosphorescence quenching (Figure 5A). The quenching of both the prompt fluorescence and phosphorescence of either Zn or Sn cyt *c* was reversed by addition of 0.6 M KCl, a condition that causes dissociation of cyt *c* from the negatively charged surfaces of poly(L-aspartate).

Since quenching was maximal at substoichiometric ratios of poly(L-aspartate) to Zn cyt *c* or Sn cyt *c*, the quenching appears to arise from interactions between closely bound cyt *c* molecules. A question arises whether the quenching could be due to a reaction between neighboring excited triplet-state cyt *c*'s (T*–T*), a type of interaction that occurs in Zn hemoglobin (Zemel & Hoffman, 1981). We observed that the computed lifetimes were the same when neutral density filters were used to attenuate the exciting light intensity by 0.5 and 0.25 times, although the light intensity of the emission was proportionately decreased. Independence of exciting light

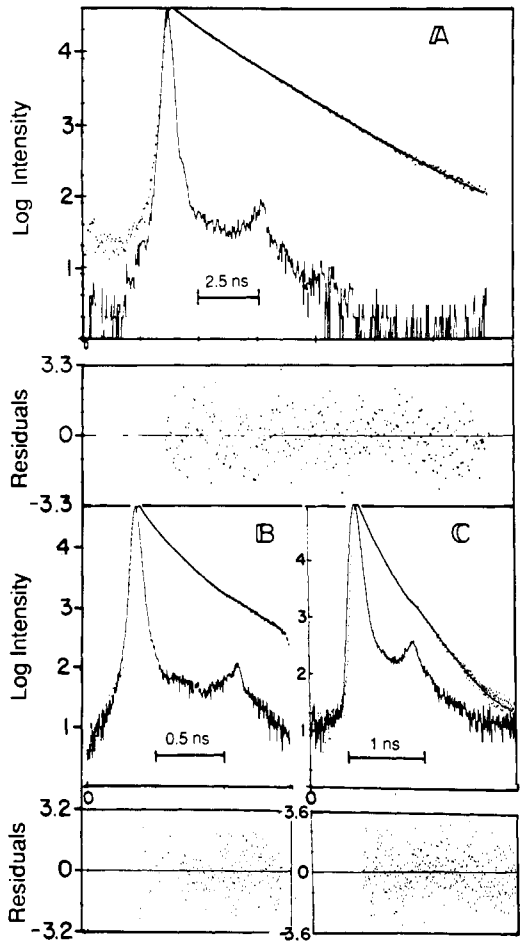


FIGURE 4: Zn and Sn cyt c fluorescence decay. (A) Fluorescence decay for Zn cyt *c*, 9.9 μM, in 10 mM potassium phosphate, pH 7.0. Excitation and emission wavelengths were 534.7 and 588 nm, respectively. Solid line through the data points represents the computed fit to three exponential functions: amplitude 0.021, lifetime 0.63 ns; amplitude 0.23, lifetime 2.4 ns; amplitude 0.1, lifetime 3.8 ns. The solid line below the data is the lamp function, on a logarithmic scale. (B) Fluorescence decay for Sn cyt *c*, 5.8 μM in 10 mM phosphate buffer, pH 7.0. Emission was monitored at 585 nm with excitation at 543 nm. The solid line is the computed fit to three exponential functions: amplitude 0.004, lifetime 1.7 ns; amplitude 0.023, lifetime 0.7 ns; amplitude 0.025, lifetime 0.1 ns. (C) Fluorescence decay for the Sn cyt *c*–CCP complex. Profiles were taken at sample concentrations of 5.8 and 10 μM for Sn cyt *c* and CCP, respectively. Excitation and emission wavelengths were as in (B). Solid line is the computed fit to three exponential functions: amplitude 0.021, lifetime 0.63 ns; amplitude 0.26, lifetime 0.022 ns; amplitude 0.0068, lifetime 1.1 ns. Lower traces for panels A–C show residuals that indicate the quality of the fit.

intensity on the decay function discounts this mechanism, as it predicts a dependency upon light intensity. Additionally, the computed lifetimes and concentration dependence of quenching were nearly the same when Zn cyt *c* was partially replaced by Fe cyt *c* (10 μM Zn cyt *c* replaced by the mixture 1 μM Zn cyt *c* and 9 μM $Fe^{2+}$ or $Fe^{3+}$, other conditions are the same as described in the legend of Figure 5). Since the excited state of Fe cyt *c* is very short (much less than a millisecond), the similar quenching profile for Zn cyt *c* and Fe cyt *c* is also incompatible with the T*–T* scheme. Therefore, under the conditions of the low light intensity of these experiments, the T*–T* reaction does not account for the observed quenching profiles.

*Luminescence of Zn CCP in the Presence of Cyt c or Poly*(L-*lysine*). No effect of ferric or ferrous cyt *c* on the prompt fluorescence yield or spectrum of Zn CCP was observed at room temperature.

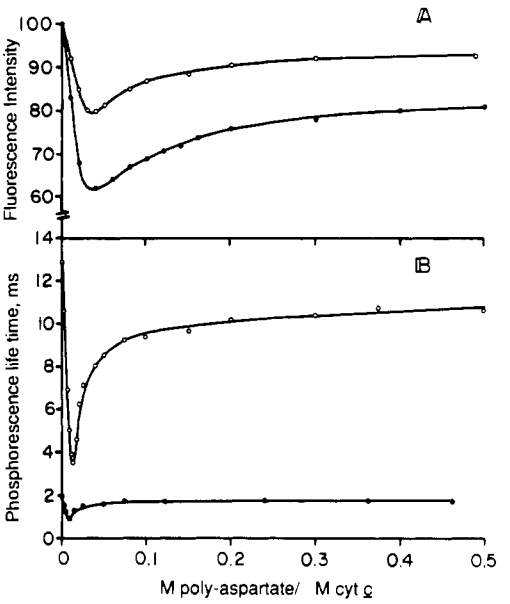


FIGURE 5: Poly(L-aspartic acid) effect on Zn cyt *c* and Sn cyt *c* luminescence at room temperature. Zn (○) and Sn (●) cyt *c*, each 5 μM, in 10 mM potassium phosphate, pH 7.0, were titrated with poly(L-aspartic acid) in the molar ratios indicated. For prompt fluorescence (A), excitation wavelengths of 423 and 396 nm and emission wavelengths of 585 and 575 were used for the Zn and Sn derivatives, respectively. Phosphorescence liftimes were measured with 423 and 405 nm as excitation and 587 and 707 nm as emission wavelengths for Zn and Sn cyt *c*, respectively (B).

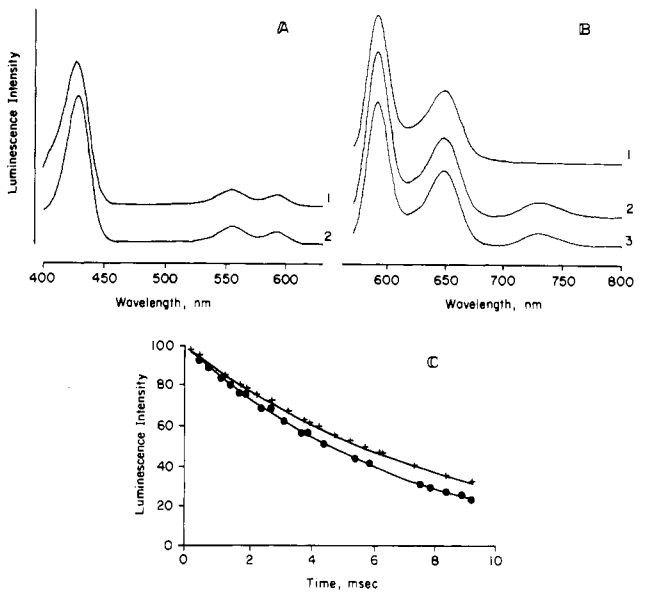


FIGURE 6: Luminescence of Zn CCP in the presence of cyt c at room temperature. (A) Excitation spectra of 0.9 μM Zn CCP (1) and 0.9 μM Zn CCP with 1.8 μM cyt *c* (2); emission wavelength 600 nm. (B) Fluorescence emission spectra of 5 μM Zn CCP (1) and delayed luminescence of 5 μM Zn CCP (2) and 5 μM Zn CCP plus 10 μM cyt *c* (3): delay time 0.2 ms; gate time 2 ms; excitation wavelength 555 nm; half-maximal band-pass 10 nm. (C) Delayed luminescence with 555 and 600 nm as excitation and emission wavelengths, respectively: (+) 5 μM Zn CCP, computer fit 8.4 ms; (●) 5 μM Zn CCP with 5 μM cyt *c*, computer fit 7.4 ms.

The Zn CCP excitation spectrum (Figure 6A) and emission spectra (Figure 6B) of phosphorescence (maximum at 738 nm) and delayed fluorescence (maximum at 602 and 655 nm) were likewise not detectably affected by the addition of cyt *c*, but the lifetime decreased from 8.4 ± 0.4 to 7.4 ± 0.3 ms upon addition of native cyt *c* (Figure 6C). These effects were the same, irrespective of the oxidation state of the iron of cyt *c*.

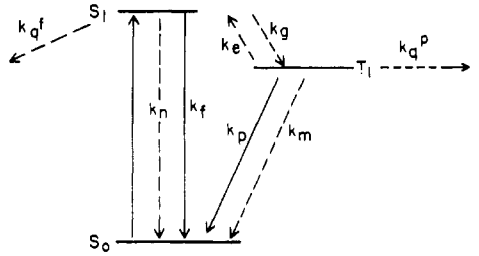


FIGURE 7: Reaction scheme. $S_0$, $S_1$, and $T_1$ represent ground, excited singlet, and excited triplet states, respectively. Dotted lines represent nonradiative transitions, and solid lines represent radiative transitions.

Because the heme of cyt *c* is covalently bound to the protein, it is impossible to test the effect of apocyt *c* on the luminescence of Zn CCP. The phosphorescence lifetime increased from 8.4 ± 0.3 to 9.1 ± 0.3 ms upon addition of molar excess poly(L-lysine), which was used to mimic the positively charged surface of cyt *c* (not shown). The increase is reversed by the addition of 0.6 M KCl, which did not affect Zn CCP phosphorescence in the absence of cyt *c*. There was no effect of substoichiometric concentrations of poly(L-lysine), unlike the case of poly(L-aspartate).

## Discussion

The transitions that we will discuss are defined in Figure 7, with solid lines denoting radiative transitions and dotted lines indicating nonradiative transitions.

Following Parker (1968), eq 5–8 define respectively the quantum efficiency of prompt fluorescence ($\Phi_f$), triplet-state formation ($\Phi_t$), phosphorescence ($\Phi_p$), and delayed fluorescence ($\Phi_e$):

$$\Phi_f = \frac{k_f}{k_f + k_n + k_g + k_q^f} \quad (5)$$

$$\Phi_t = \frac{k_g}{k_f + k_n + k_g + k_q^f} \quad (6)$$

$$\Phi_p = \frac{k_p \Phi_t}{k_p + k_m + k_e + k_q^p} \quad (7)$$

$$\Phi_e = \frac{k_e \Phi_f \Phi_t}{k_p + k_m + k_e + k_q^p} \quad (8)$$

where $k_q^f$ and $k_q^p$ are the rate constants for the quenching of the $S_1$ and $T_1$ excited-state molecules, respectively, by an exogeneous quencher (CCP being the quencher in the pairs Zn cyt *c*–CCP and Sn cyt *c*–CCP or cyt *c* in the pair Zn CCP–cyt *c*).

The observed fluorescence ($\tau_f$) and phosphorescence ($\tau_p$) lifetimes are related to the rate constants by eq 9 and 10.

$$\tau_f = \frac{1}{k_f + k_n + k_g + k_q^f} \quad (9)$$

$$\tau_p = \frac{1}{k_p + k_m + k_e + k_q^p} \quad (10)$$

The determined and calculated values of quantum efficiencies, rate constants, and lifetimes are presented in Table I.

*Distance Calculations between Cyt c and CCP.* Zn cyt *c* and Sn cyt *c* were quenched by CCP; Zn CCP was not quenched by cyt *c*. The fluorescence emission of Zn protoporphyrin in CCP was at 602 nm, and there was negligible spectral overlap with cyt *c* absorption. Spectral overlap did exist between the emission of Zn or Sn cyt *c* (a type of metalloporphyrin with emission at 588 and 578 nm, respectively) and CCP. The rate constants, $k_q^f$, of energy transfer from the singlet excited state of Zn cyt *c* or Sn cyt *c* to CCP are $8.4 \times 10^7$ and $3.2 \times 10^8$ $s^{-1}$, respectively (Table I). On the basis of spectral overlap between Zn or Sn cyt *c* and CCP and the calculated $k_q^f$ value, the distance between the porphyrin on the cytochrome *c* derivatives is 1.8–1.9 nm according to the Förster theory (eq 1). The Förster theory assumes point sources, and therefore, it is not clear whether this refers to the edge-to-edge or center-to-center distance. Molecular models based upon crystallographic studies suggest that 1.8 nm is the closest approach of the two heme edges and 2.5 nm for the two iron atoms (Poulos & Kraut, 1980; Poulos & Finzel, 1984). The relative long distance between the two redox centers correlates well with the one measured by Leonard and Yonetani (1974) between protoporphyrin apoCCP and ferric/ferrous cyt *c* using a fluorescence/tryptophan phosphorescence at 77 K technique (1.7–2.0 nm). Nuclear magnetic resonance studies (Gupta & Yonetani, 1973) also showed that cyt *c* and CCP hemes in the complex are relatively far from each other (>2.5 nm), assuming the electronic relaxation time of the high-spin iron in CCP to be ca. $10^{-10}$ s.

Table I: Quantum Efficiencies, Lifetimes, and Rate Constants for Processes in Zn Cyt *c*, Sn Cyt *c*, Zn Cyt *c*–CCP, and Sn Cyt *c*–CCP[a]

| | Zn cyt *c* | Zn cyt *c*–CCP | Sn cyt *c* | Sn cyt *c*–CCP |
|---|---|---|---|---|
| $\Phi_f$ | 0.055[b] | 0.044 | 0.012[b] | 0.0077 |
| $\Phi_t$ | 0.9[b] | 0.72 | 0.95[b] | 0.61 |
| $\Phi_p$ | 0.0044[b] | $5 \times 10^{-4}$ | $4 \times 10^{-3}$ [b] | $9.3 \times 10^{-4}$ |
| $\Phi_e$ | 0.0044[b] | 0.00204 | 0.0014[b] | $5.8 \times 10^{-4}$ |
| $\tau_p$ (s) | 0.014 | 0.0015 | 0.003 | 0.0011 |
| $\tau_f$ (s) | $3 \times 10^{-9}$ | $2.4 \times 10^{-9}$ | $1.7 \times 10^{-9}$ | $1.1 \times 10^{-9}$ |
| $k_f$ ($s^{-1}$) | $1.8 \times 10^7$ | $1.8 \times 10^7$ | $7 \times 10^6$ | $7.0 \times 10^6$ |
| $k_p$ ($s^{-1}$) | 0.35 | 0.44 | 1.5 | 1.4 |
| $k_e$ ($s^{-1}$) | 6.3 | 41 | 41 | 41 |
| $k_g$ ($s^{-1}$) | $3.0 \times 10^8$ | $3.0 \times 10^8$ | $5.5 \times 10^8$ | $5.5 \times 10^8$ |
| $k_n$ ($s^{-1}$) | $1.5 \times 10^7$ | $1.5 \times 10^7$ | $2.2 \times 10^7$ | $2.2 \times 10^7$ |
| $k_m$ ($s^{-1}$) | 64.7 | 64.7 | 297 | 297 |
| $k_q^f$ ($s^{-1}$) | | $8.4 \times 10^7$ | | $3.2 \times 10^8$ |
| $k_q^p$ ($s^{-1}$) | | 519 | | 570 |

[a] Conditions given under Materials and Methods. Temperature: 20–22 °C. [b] Values taken from Dixit et al. (1984).

*Effects of ApoCCP/CCP Binding to Zn Cyt c and Sn Cyt c: "Conformational" and "Electronic" Effects on Phosphorescence.* The binding of CCP or apoCCP to Zn cyt *c* causes a 20-nm shift in the phosphorescence spectrum of the latter (Figure 1 and inset). The spectral shift (from 738 to 718 nm) is identical in the presence or absence of the heme in CCP; therefore, it must arise from a change in the environment of Zn cyt *c* porphyrin induced by the polypeptide chain of CCP. One explanation for the shift to lower emission maximum would be an increased torsion or bending of the Zn cyt *c* porphyrin ring in the protein, which does not seem to affect the shorter lived fluorescence. Interestingly, Sn cyt *c* has no such detectable shift in the phosphorescence emission upon binding of CCP (Figure 1B). We note that Hoard (1971) differentiates between the stereochemistry of model Zn and Sn porphyrins. The Sn porphyrin molecule in the crystal state is $C_{4h}$ (with tetragonal symmetry), but the precisely determined parameters are fully compatible with $D_{4h}$ symmetry for the unconstrained molecule. However, Zn porphyrins are square-pyramidal five-coordinated structures ($C_{4v}$). The chemical sensitivity of Zn cyt *c* compared to Sn cyt *c* is also manifested by (a) quick photodecomposition in the presence of oxygen and (b) relative ease of removal of the metal from the Zn chelates (Vanderkooi et al., 1976). Both phenomena could be related to strain at the nitrogen–Zn bond

and perhaps readier proton attack at the nitrogen atoms.

Our experiments showed that CCP quenches the fluorescence of Zn cyt *c* and Sn cyt *c*, shifts the phosphorescence maximum of Zn cyt *c*, and quenches the phosphorescence of both derivatives. The rate constant $k_q^P$ for the quenching of Zn cyt *c* and Sn cyt *c* phosphorescence by CCP is 519 and 570 $s^{-1}$, respectively (Table I). ApoCCP itself partially quenches Zn cyt *c* phosphorescence (Figure 2B). From these observations we conclude that the phosphorescence quenching of Zn cyt *c* is composed of a "conformational" effect as well as an "electronic" effect, with different rate constants. As apoCCP does not affect the fluorescence yield of Zn cyt *c* (Figure 2A, inset), we assumed that the yield of the triplet state, $\Phi_t$, is unchanged for Zn cyt *c* and the Zn cyt *c*–apoCCP complex. Using this approximation, we obtain the relationships

$$k_{conf} = \frac{k_p \Phi_t}{\Phi_p} - k_p - k_m - k_e \quad (11)$$

and

$$k_{elect} = k_q^f - k_{conf} \quad (12)$$

where $k_{conf}$ expresses a rate constant for quenching of Zn cyt *c* by apoCCP (without the heme present) and $k_{elect}$ is the rate constant for the electronic effect. For the Zn cyt *c*–CCP couple, the electronic rate constant has a value of 458 $s^{-1}$, whereas the rate constant for the conformational effect is 61 $s^{-1}$.

*Effect of Poly(L-aspartate) on Zn Cyt c and Sn Cyt c.* Because of the suggestion that aspartates on CCP interact with lysines on cyt *c* upon complexing, we studied the effect of poly(L-aspartate) on Zn cyt *c* and Sn cyt *c*. The interaction of these proteins with poly(L-aspartate) (Figure 5) was complex: at very low ratios of poly(L-aspartate) to cyt *c*, quenching of prompt fluorescence and a decrease in phosphorescence lifetime occurred. Upon increasing the ratio of poly(L-aspartate) to the cyt *c* derivative, both parameters increased; it therefore appears that the interaction is occurring between closely bound cyt *c* molecules. Because spectral overlap occurs between the absorption and emission spectra of these cyt *c* derivatives, a mechanism for the fluorescence quenching could be singlet energy transfer of the long-range Förster type. For the phosphorescence quenching we excluded a T*–T* reaction and conclude that the triplet excited-state Zn and Sn cyt *c* can interact with the ground-state molecule. Because the central metals are closed shell, electron transfer/exchange must involve only the electrons of the porphyrin ring.

In principle, the quenching of the fluorescence of Zn cyt *c* and Sn cyt *c* by CCP or by the ground-state donor molecule [as in the presence of poly(L-aspartate)] could affect the phosphorescence lifetime, because thermal repopulation of the singlet state from the triplet state provides another decay route for the triplet (Figure 7). This back-reaction rate constant, $k_e$, is 6.3 and 41 $s^{-1}$ for Zn cyt *c* and Sn cyt *c*, respectively (Table I). For the case of CCP binding to Zn cyt *c*, the phosphorescence spectrum of the Zn porphyrin shifts to the blue upon addition of CCP (Figure 1); therefore, the back-reaction rate changes. The following equation gives the relationship between rate constants and spectral energy differences:

$$k_e^{II} = k_e^{I} \frac{e^{-\Delta E^{II}/RT}}{e^{-\Delta E^{I}/RT}} \quad (13)$$

where $E^I$ and $E^{II}$ are the differences in energy between the fluorescence emission maximum and the phosphorescence emission maximum of Zn cyt *c* in the presence and absence of CCP, respectively. We can calculate that the rate constant of the back-reaction becomes 41 $s^{-1}$ in Zn and Sn cyt *c* in the presence of CCP. (Sn cyt *c* and Sn cyt *c*–CCP have the same $k_e$ = 41 $s^{-1}$, as CCP does not shift the phosphorescence spectrum maximum). Because the back-rate is very slow, we can neglect the effect of quenching of the singlet state on the phosphorescence lifetime, irrespective of whether the spectra changed or not.

It was observed that upon incremental additions of poly(L-aspartate) to Zn cyt *c* or Sn cyt *c* the phosphorescence lifetime recovered before the fluorescence yield (Figure 5). This experimentally shows that quenching of fluorescence does not account for the phosphorescence quenching. The difference in the recovery profiles for phosphorescence lifetime and fluorescence yield may be due to different distance dependencies for singlet and triplet transfer.

*Effects of Cyt c Binding to Zn CCP: Conformational and Electronic Effect on Phosphorescence Rate Constants.* The phosphorescence lifetime of Zn CCP decreased from 8.4 to 7.4 ms in the presence of cyt *c* (Figure 6C). This change corresponds to a quenching rate constant, $k_q^P$, of 17 $s^{-1}$. However, in the presence of the polycation poly(L-lysine), the lifetime of Zn CCP increased from 8.4 to 9.1 ms. This rather small effect could be due to shielding of the Zn CCP porphyrin from quenchers in the medium. If cyt *c* offers the same protection, then the rate constant $k_q^P$ is 25.2 $s^{-1}$ (for the decrease in lifetime from 9.1 to 7.4 ms). This value is comparable to the rate of electron transfer from the triplet state of Zn CCP to cyt *c* within the complex [$k_t$ = 25 $s^{-1}$ for tuna cyt *c* (Liang et al., 1986) or $k_t$ = 17 $s^{-1}$ for horse cyt *c* (Ho et al., 1985)].

*Comparison of the Binding of CCP to Zn/Sn Cyt c with Cyt c Binding to Zn CCP.* In each case of triplet quenching (the Zn/Sn cyt *c* triplet quenching by CCP and by their respective ground-state molecules or Zn CCP triplet by cyt *c*), spectral overlap between the triplet-state emission and the absorption of the acceptor either does not exist or is very small. Therefore, long-range transfer of the dipolar type is excluded, and an electron exchange or transfer is the likely mechanism of quenching. The quenching of phosphorescence means that electron transfer/exchange can occur over long distances in the extended lifetime of the triplet excited state; this interpretation is in agreement with that of other workers (Simolo et al., 1984; Peterson-Kennedy et al., 1986; Ho et al., 1985; McLendon et al., 1985). Because in our work the disappearance of the reactant was monitored, we cannot differentiate between electron exchange and electron transfer with fast electron recombination in the ground state. The two mechanisms could be distinguished by transient absorption or electron paramagnetic resonance measurements. In similar systems, quenching of Zn cyt *c* by cyt $b_5$ was attributed to electron transfer (McLendon et al., 1985).

The rate constant for the quenching of Zn CCP by cyt *c*, $k_{elect}$ = 20 $s^{-1}$, is dramatically smaller than for the complementary pair Zn cyt *c*–CCP with $k_{elect}$ = 458 $s^{-1}$. The porphyrin in CCP is protoporphyrin IX, which has a vinyl group, and the porphyrin in cyt *c* is a mesoporphyrin type; this difference may be enough to change the energy levels to make transfer more favorable in one direction. The protein polypeptide chain is also implicated in the directionality. Intramolecular electron-transfer assymetry has recently been observed in the model system of cyt *c*–ruthenium complex, where ruthenium complex is specifically bound at the imidazole moiety of a surface-exposed histidine (Bechtold et al., 1986). This has been interpreted in terms of fast conformational changes of the protein that affect the electron-transfer di-

rectionality. In this case, the pathways for reduction and oxidation of the same center are probably different, whereas the driving forces are equal for both ways. A conformational difference between the redox partners is indicated by the change in the phosphorescence spectrum of Zn cyt *c*, but not Zn CCP, when the redox partner binds; therefore, the binding of cyt *c* does not affect the porphyrin environment of Zn CCP in the way that CCP interacts with the porphyrin of Zn cyt *c*.

In summary, this study on the fluorescence and phosphorescence of metal (Zn and Sn) derivatives of cyt *c* and CCP reconfirms with fluorescence quenching measurements earlier estimations of the rather long distance between the two protein chromophores. Phosphorescence quenching data show that the two heme proteins are influenced both by conformational effects, induced by binding of the redox partner, and by direct electronic effects of neighboring porphyrins. Electronic effects are observed in these couples: Zn cyt *c*–CCP, Sn cyt *c*–CCP, and Zn CCP–cyt *c*. Electronic effects are also observed between excited-state and ground-state Zn cyt *c* and Sn cyt *c* molecules when they are bound to poly(L-lysine). Conformational effects can be clearly distinguished from electronic effects, and the respective rate constants have been assigned.

ACKNOWLEDGMENTS

We thank Dr. G. Holtom of the Regional Laser Laboratory for assistance in fluorescence lifetime measurements.

REFERENCES

Bechtold, R., Kuehn, C., Lepre, C., & Isied, S. (1986) *Nature (London) 322*, 286–288.

Calhoun, D. B., Vanderkooi, J. M., Woodrow, G. V., III, & Englander, S. W. (1983) *Biochemistry 22*, 1526–1532.

Cheung, E., Taylor, K., Kornblatt, J. A., English, A. M., McLendon, G., & Miller, J. R. (1986) *Proc. Natl. Acad. Sci. U.S.A. 83*, 1330–1333.

Dale, R. E., Eisinger, J., & Blumberg, W. E. (1979) *Biophys. J. 26*, 161–194.

Dixit, B. P. S. N., Moy, V. T., & Vanderkooi, J. M. (1984) *Biochemistry 23*, 2103–2107.

Förster, T. (1959) *Discuss. Faraday Soc. 27*, 7–17.

Gupta, R. K., & Yonetani, T. (1973) *Biochim. Biophys. Acta 292*, 502–508.

Ho, P. S., Sutoris, C., Liang, N., Margoliash, E., & Hoffman, B. M. (1985) *J. Am. Chem. Soc. 107*, 1070–1071.

Hoard, J. L. (1971) *Science (Washington, D.C.) 174*, 1295–1302.

Leonard, J. J., & Yonetani, T. (1974) *Biochemistry 13*, 1465–1468.

Leonard, J. J., Yonetani, T., & Callis, J. B. (1974) *Biochemistry 13*, 1460–1464.

Liang, N., Kang, C. H., Ho, P. S., Margoliash, E., & Hoffman, B. M. (1986) *J. Am. Chem. Soc. 108*, 4665–4666.

McLendon, G., & Miller, J. R. (1985) *J. Am. Chem. Soc. 107*, 7811–7816.

McLendon, G. L., Winkler, J. R., Noccera, D. G., Mauk, M. R., Mauk, A. G., & Gray, H. B. (1985) *J. Am. Chem. Soc. 107*, 739–740.

Parker, C. A. (1968) *Photoluminescence of Solutions*, pp 71–108, Elsevier, New York.

Parker, C. A., & Hatchard, C. G. (1961) *Trans. Faraday Soc. 57*, 1814–1904.

Peterson-Kennedy, S. E., McGourty, J. L., Kalweit, J. A., & Hoffman, B. M. (1986) *J. Am. Chem. Soc. 108*, 1739–1746.

Poulos, T. L., & Kraut, J. (1980) *J. Biol. Chem. 255*, 10322–10330.

Poulos, T. L., & Finzel, B. C. (1984) *Pept. Protein Rev. 4*, 115–171.

Poulos, T. L., Freer, S. T., Alden, R. A., Edwards, S. L., Sloglund, U., Takio, K., Eriksson, B., Xuong, N.-H., Yonetani, T., & Kraut, J. (1980) *J. Biol. Chem. 255*, 575–580.

Sinolo, K. P., McLendon, G. L., Mauk, M. R., & Mauk, A. G. (1984) *J. Am. Chem. Soc. 106*, 5012–5013.

Takano, T., Kallai, O. B., Swanson, R., & Dickerson, R. E. (1973) *J. Biol. Chem. 248*, 5235–5255.

Turro, N. J. (1978) in *Modern Molecular Photochemistry*, pp 296–361, Benjamin/Cummings, Menlo Park, CA.

Vanderkooi, J. M., Adar, F., & Erecinska, M. (1976) *Eur. J. Biochem. 64*, 381–387.

Vanderkooi, J. M., Landesberg, R., Hayden, G. W., Owen, C. S. (1977) *Eur. J. Biochem. 81*, 339–347.

Vanderkooi, J. M., Glatz, P., Casadei, J., & Woodrow, G. V., II (1980) *Eur. J. Biochem. 110*, 189–196.

Yonetani, T. (1967) *J. Biol. Chem. 242*, 5008–5013.

Yonetani, T., & Ray, G. S. (1965) *J. Biol. Chem. 240*, 4503–4508.

Yonetani, T., & Asakura, T. (1968) *J. Biol. Chem. 243*, 3996–3998.

Zemel, H. E., & Hoffman, B. M. (1981) *J. Am. Chem. Soc. 103*, 1192–1201.